Title

Effect of bay K 8644 (-) and the beta2a subunit on Ca2+-dependent inactivation in alpha1C Ca2+ channels.

Journal

The Journal of general physiology, 111(3)

ISSN

0022-1295

Authors

Noceti, F
Olcese, R
Qin, N
et al.

Publication Date

1998-03-01

DOI

10.1085/jgp.111.3.463

Peer reviewed

Effect of Bay K 8644 (−) and the β_{2a} Subunit on Ca^{2+}-dependent Inactivation in α_{1C} Ca^{2+} Channels

Francesca Noceti,* Riccardo Olcese,* Ning Qin,* Jianming Zhou,* and Enrico Stefani*‡§

From the *Department of Anesthesiology, and ‡Department of Physiology, School of Medicine, University of California, Los Angeles, Los Angeles, California 90095-1778; and §Conicet, Buenos Aires, Argentina 1033

ABSTRACT Ca^{2+} currents recorded from *Xenopus* oocytes expressing only the α_{1C} pore-forming subunit of the cardiac Ca^{2+} channel show Ca^{2+}-dependent inactivation with a single exponential decay. This current-dependent inactivation is not detected for inward Ba^{2+} currents in external Ba^{2+}. Facilitation of pore opening speeds up the Ca^{2+}-dependent inactivation process and makes evident an initial fast rate of decay. Facilitation can be achieved by (*a*) coexpression of the β_{2a} subunit with the α_{1C} subunit, or (*b*) addition of saturating Bay K 8644 (−) concentration to α_{1C} channels. The addition of Bay K 8644 (−) to $\alpha_{1C}\beta_{2a}$ channels makes both rates of inactivation faster. All these maneuvers do not induce inactivation in Ba^{2+} currents in our expression system. These results support the hypothesis of a mechanism for the Ca^{2+}-dependent inactivation process that is sensitive to both Ca^{2+} flux (single channel amplitude) and open probability. We conclude that the Ca^{2+} site for inactivation is in the α_{1C} pore-forming subunit and we propose a kinetic model to account for the main features of $\alpha_{1C}\beta_{2a}$ Ca^{2+} currents.

KEY WORDS: Ca^{2+} currents • decay • *Xenopus* • subunit • kinetic model

INTRODUCTION

Regulation of Ca^{2+} currents by Ca^{2+} influx includes a negative feedback mechanism that inactivates the current itself when Ca^{2+} is the charge carrier. Currents elicited by depolarizing steps show a fast activating phase followed by a Ca^{2+}-dependent inactivating phase. This feature has been extensively studied in native channels (Eckert and Chad, 1984; Chad, 1989; Gutnick et al., 1989; Kostyuk, 1992; Shirokov at el., 1993) and has been recently demonstrated in cloned channels (Neely et al., 1994; Zong et al., 1996; de Leon et al., 1995). It has been shown that Ca^{2+} chelators can reduce the efficiency of the inactivation process (Imredy and Yue, 1992; Haack and Rosenberg, 1994) and that the Ca^{2+} influx through a channel can contribute to the inactivation of adjacent channels (cross talk) (Mazzanti et al., 1991; Imredy and Yue, 1992; Galli et al., 1994). These results suggested the presence of a specific Ca^{2+} site on the intracellular face of the channel protein (Huang et al., 1989). Two questions emerge: (*a*) Is the α_{1C} pore-forming subunit alone capable of Ca^{2+}-dependent inactivation, or, on the contrary, is the accessory β_{2a} subunit required (Neely et al., 1994; Zong et al., 1996)? (*b*) Is this inactivating process related to intracellular Ca^{2+} build-up (Chad et al., 1984; Mazzanti et al., 1991), or does Ca^{2+} entry through a single channel inactivate the same channel by a Ca^{2+} regulatory site located deep inside the pore (Yue et al., 1990)?

To address these questions, we performed whole cell experiments with the cut-open oocyte Vaseline gap technique (Stefani et al., 1994) on *Xenopus* oocytes expressing the cloned α_{1C} subunit of the rabbit cardiac Ca^{2+} channel, with and without the accessory β_{2a} subunit (Neely et al., 1994). Ca^{2+} and Ba^{2+} currents were recorded in oocytes after the intracellular injection of the fast Ca^{2+} chelating agent Na_4-BAPTA (1,2-bis(*o*-aminophenoxy)-ethane-*N*,*N*,*N*′,*N*′-tetraacetate, $K_{on} = 6 \times 10^8\ M^{-1}\,s^{-1}$) to prevent contaminant Ca^{2+}-activated Cl^- currents (Neely et al., 1994). The action of the dihydropyridine (DHP)[1] agonist Bay K 8644 (−) on the inactivation rates was also investigated, since this agent increases the size of the macroscopic current by changing the channel open probability without significantly changing the single channel amplitude (Hess et al.,

J. Zhou's current address is Zeneca Pharmaceuticals, Wilmington, DE 19897.

Address correspondence to Dr. Enrico Stefani, UCLA, Dept. of Anesthesiology, BH-612 CHS, Box 951778, Los Angeles, CA 90095-1778. Fax: 310-825-6649; E-mail: estefani@ucla.edu

[1]*Abbreviations used in this paper:* DHP, dihydropyridine; HP, holding potential; I-V, voltage dependencies of current; r-V, voltage dependencies of rate of inactivation; SHP, subtracting holding potential.

1984). In this respect, the effect of Bay K 8644 (−) would mimic the effect of the β_{2a} subunit.

We found that Ca^{2+} currents from the α_{1C} subunit expressed alone can inactivate in a Ca^{2+}-dependent manner. The single exponential fits to these currents have time constants that decrease when the Ca^{2+} concentration is increased. The coexpression of the β_{2a} subunit makes evident a double exponential decay with a faster time course and with rates that are Ca^{2+} dependent. Similarly, the addition of saturating concentrations of Bay K 8644 (−) to α_{1C} channels induces the appearance of the fast rate of Ca^{2+}-dependent inactivation. These results confirm the view that the Ca^{2+} binding site for the inactivation is part of the pore-forming α_{1C} subunit (Neely et al., 1994; de Leon et al., 1995; Zhou et al., 1997) and is located in a region very close to the inner mouth pore, within a microdomain where the local Ca^{2+} concentration can reach its steady state in a few microseconds. Based on the fact that the rates of Ca^{2+}-dependent inactivation are sensitive to both Ca^{2+} flux through the channel (single channel current) and open probability, we propose a kinetic model for the Ca^{2+}-dependent inactivation process in $\alpha_{1C}\beta_{2a}$ channels.

MATERIALS AND METHODS

RNA Synthesis and Oocyte Injection

The plasmids containing cDNA fragments encoding the cardiac α_{1C} and β_{2a} subunits were digested with HindIII (Wei et al., 1991). The linearized templates were treated with 2 μg proteinase K and 0.5% SDS at 37°C for 30 min, and then twice extracted with phenol/chloroform, precipitated with ethanol, and resuspended in distilled water to a final concentration of 0.5 μg/μl. The cRNAs were transcribed from 0.5 μg of linearized DNA template at 37°C with 10 U of T7 RNA polymerase (Boehringer Mannheim Biochemicals, Indianapolis, IN), in a volume of 25 μl containing 40 mM Tris-HCl (pH 7.2), 6 mM $MgCl_2$, 10 mM dithiothreitol, 0.4 mM each of ATP, GTP, CTP, and UTP, 0.8 mM 7-methyl-GTP. The transcription products were extracted with phenol and chloroform, twice precipitated with ethanol and resuspended in double distilled water to a final concentration of 0.2 μg/μl, and 50 nl were injected per oocyte. Before injection, oocytes were defolliculated by collagenase treatment (type I, 2 mg/ml for 40 min at room temperature; Sigma Chemical Co., St. Louis, MO). Oocytes were maintained at 19.0°C in Barth solution. Recordings were done 4–12 d after RNA injection.

Recording Technique and Solutions

Recording of macroscopic current was performed using the cut-open oocyte Vaseline gap technique (Stefani et al., 1994) on *Xenopus laevis* oocytes. The oocyte was placed in a triple compartment perspex chamber; voltage clamped currents were recorded from the top chamber, while the middle chamber (set at the same voltage as the recording chamber) isolated the top from the bottom chamber. The oocyte membrane exposed to the bottom chamber was permeabilized with 0.1% saponin in the internal saline (see bottom chamber solution). Microelectrodes probing voltage across the membrane (top chamber) had a resistance of ~0.5–1 MΩ, and they were filled with (M): 2.7 NaMES (Na-methanesulfonic acid), 0.01 Na_2-EGTA, 0.01 NaCl. Holding potential was −90 mV. All experiments were performed at room temperature. Subtraction of linear components was digitally obtained by scaled currents elicited by small control pulses of one-fourth the amplitude of the stimulating pulse (P/−4). Acquisition and data analysis were done on a personal computer. Signals were filtered at one-fifth the sampling frequency.

External solutions, used in the top and guard compartments were: NaMESBa-10 (10 mM BaOH; 96 mM NaMES; 10 mM HEPES, titrated to pH 7.0 with CH_3SO_3H), NaMESCa-2, -5, or -10 (2, 5, or 10 mM CaOH, 102 mM NaMES, 10 mM HEPES, titrated to pH 7.0 with CH_3SO_3H), or NMGMESCa-10 (10 mM Ca^{2+}, 96 mM *N*-methyl-D-glucamine [NMG^+], 10 mM HEPES, titrated to pH 7.0 with CH_3SO_3H). The solution in the bottom chamber in contact with the oocyte cytoplasm was 110 mM K-glutamate (10 mM HEPES, titrated to pH 7.0 with KOH). Na_4-BAPTA (tetrasodium-1,2-bis (*o*-aminophenoxy)-ethane-*N,N,N′,N′*-tetraacetate) was loaded into a glass micropipette of ~20-μm tip diameter, and ~100 nl were injected with an automatic microinjector immediately before mounting the oocyte in the recording chamber. Na_4-BAPTA stock solutions of 50 mM were made in distilled water and titrated at pH 7.0 with CH_3SO_3H. The BAPTA injections were performed before the experiments to prevent contamination of Ca^{2+} currents with Ca^{2+}- and Ba^{2+}-activated Cl^- currents (Miledi, 1982; Barish, 1983; Neely et al., 1994). This BAPTA concentration selectively eliminated Cl^- currents without any significant action on Ca^{2+}-dependent current decay (Neely et al., 1994). To probe the accessibility of the internal Ca^{2+} site, we had to dramatically increase the internal BAPTA concentration (500 mM BAPTA and 10 mM NaCl) and to continuously perfuse the oocytes (1 ml/h) via a glass pipette inserted into the bottom side of the oocyte.

Values for the rates of Ca^{2+}-dependent inactivation were obtained by fitting to a double exponential ($\alpha_{1C}\beta_{2a}$; α_{1C} in the presence of 500 nM Bay K 8644 (−)) or to a single exponential (α_{1C}) the decay of the Ca^{2+} current (from the peak of the current up to 800 ms). The exponential functions were

$$P + \sum_{i=1}^{n} A_i e^{-\frac{t}{\tau_i}}$$

with $n = 1$ and 2. P was the offset factor, and A_i the amplitude of each exponential component.

The model-fitting procedure was implemented with SCoP (Simulation Resources, Inc., Barren Springs, MI). The rates in the transitions were exponential functions of the voltage, as predicted by the Eyring theory. Simultaneous fitting of current traces at different potentials was performed to evaluate the kinetic parameters in a non–steady state model. The source file, containing a system of differential equations, was compiled and the resulting executable file was fed with ensembles of current recordings under different conditions, such as subunit expression, Ca^{2+} concentration, and presence of the DHP agonist Bay K 8644 (−).

RESULTS

Ca^{2+}-dependent Inactivation in α_{1C}-expressing Oocytes

Fig. 1 shows Ba^{2+} and Ca^{2+} currents (*left* and *right*, respectively) recorded from an oocyte expressing the α_{1C} subunit alone. The currents were elicited by depolarizing pulses from a holding potential of −90 mV. The figure shows that, during large depolarizing pulses, Ba^{2+} currents had a very slow decay, while Ca^{2+} currents showed a much faster decay that could be attributed to

the Ca^{2+}-dependent inactivation process. The decay phase of the currents was fitted to a single exponential function of the form $Ae^{-tr} + C$, where A is the amplitude factor, t the time, r the rate, and C the offset. The fit was for Ba^{2+} (Fig. 1 *A*): $A = -4.1$ nA, $r = 0.001$ ms^{-1} and $C = -17.9$ nA at 0 mV and for Ca^{2+} (Fig. 1 *B*): $A = -4.5$ nA, $r = 0.003$ ms^{-1}, and $C = -4.8$ nA at 0 mV. The relative amplitude factor, $A/(A + C)$, was larger and the rate of decay was much faster in external Ca^{2+}. This difference in the decay phase between Ca^{2+} and Ba^{2+} currents became more evident after potentiating the Ca^{2+} current by adding a submaximal concentration (50 nM) of the DHP agonist Bay K 8644 (−). The potentiated Ba^{2+} currents had a similar time course to the control (compare Fig. 1, *C* and *A*). Thus, Ba^{2+} does not substitute Ca^{2+} for the inactivation in the time scale used (0.5–1 s). During the time course of our experiments, the main effect of Bay K 8644 was to potentiate Ba^{2+} currents. On the other hand, in external Ca^{2+}, Bay K 8644 induced an increase in the size of the peak current as well as an increase in the decay (Fig. 1, *B* and *D*). Thus, facilitation of pore opening by Bay K 8644 (−) makes more evident Ca^{2+}-dependent inactivation, which is already present in the absence of the agonist.

Effect of the β_{2a} Subunit on α_{1C} Currents

Fig. 2 shows the effect of coexpression of the β_{2a} subunit with the α_{1C} subunit on the rates of Ca^{2+}-dependent inactivation. Ba^{2+} and Ca^{2+} currents (Fig. 2, *left* and *right*, respectively) in oocytes coexpressing the pore-forming α_{1C} subunit together with the regulatory β_{2a} subunit had faster activation rates and larger amplitudes than in oocytes expressing the α_{1C} subunit alone. This is expected from the facilitation of the pore opening by the coexpression of the β_{2a} subunit. By comparing the recordings in external Ca^{2+} (Figs. 1 and 2, *right*), it becomes evident that the β_{2a} subunit speeds up the Ca^{2+}-dependent inactivation process (Fig. 2, *B* and *D*). As was the case for α_{1C} currents, in $\alpha_{1C}\beta_{2a}$, the addition of a submaximal concentration of Bay K 8644 (−) (50 nM) increased both Ba^{2+} and Ca^{2+} current amplitudes. From these results we can conclude that maneuvers that increase the open probability of the Ca^{2+} channel without affecting the single channel amplitude (addition of Bay K 8644 (−) and the coexpression of the β_{2a} subunit; Costantin et al., 1995) speed up the Ca^{2+}-dependent inactivation process.

In addition to the Ca^{2+}-dependent inactivation phase, both α_{1C} and $\alpha_{1C}\beta_{2a}$ currents show a slow smaller component of inactivation that is weakly voltage dependent. This slow inactivation is more clearly detected in Ba^{2+} currents (Figs. 1, *A* and *C*, and 2, *A* and *C*) since, in external Ca^{2+}, the Ca^{2+} inactivation process predominates. This slower component can be attributed to a slow voltage-dependent inactivation (Lee et al., 1985;

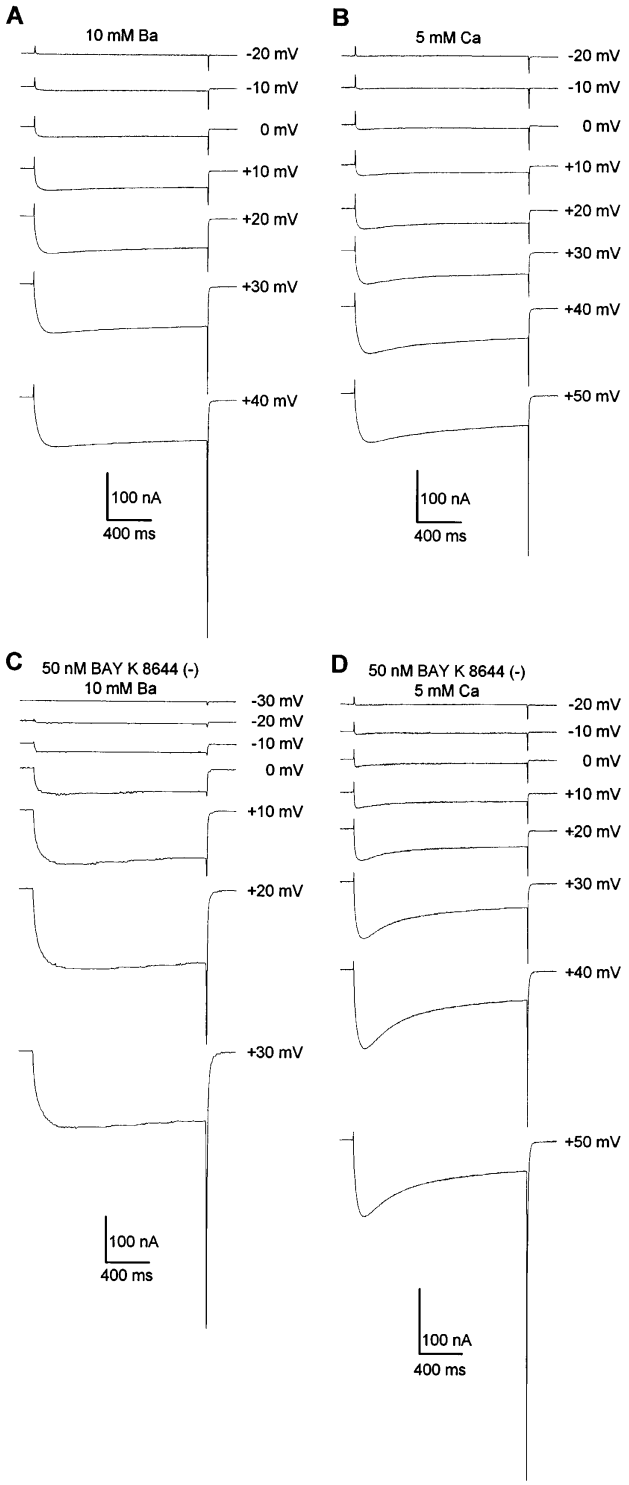

FIGURE 1. Ca^{2+}-dependent inactivation of Ca^{2+} current in the cloned α_{1C} subunit of a cardiac Ca^{2+} channel. Families of traces evoked by 1,600-ms depolarizing steps from a holding potential of −90 mV in an oocyte expressing the α_{1C} subunit alone, and the effect of DHP agonist Bay K 8644 (−). (*A*) Voltage steps from −90 mV, Ba^{2+} was the charge carrier (10 mM Ba^{2+}). (*B*) Traces recorded in 5 mM Ca^{2+}. (*C*) Ba^{2+} currents recorded in the presence of 50 nM Bay K 8644 (−). (*D*) Ca^{2+} currents recorded in the presence of 50 nM Bay K 8644 (−). Linear components were digitally subtracted by subpulses from the holding potential using the P/−4 method.

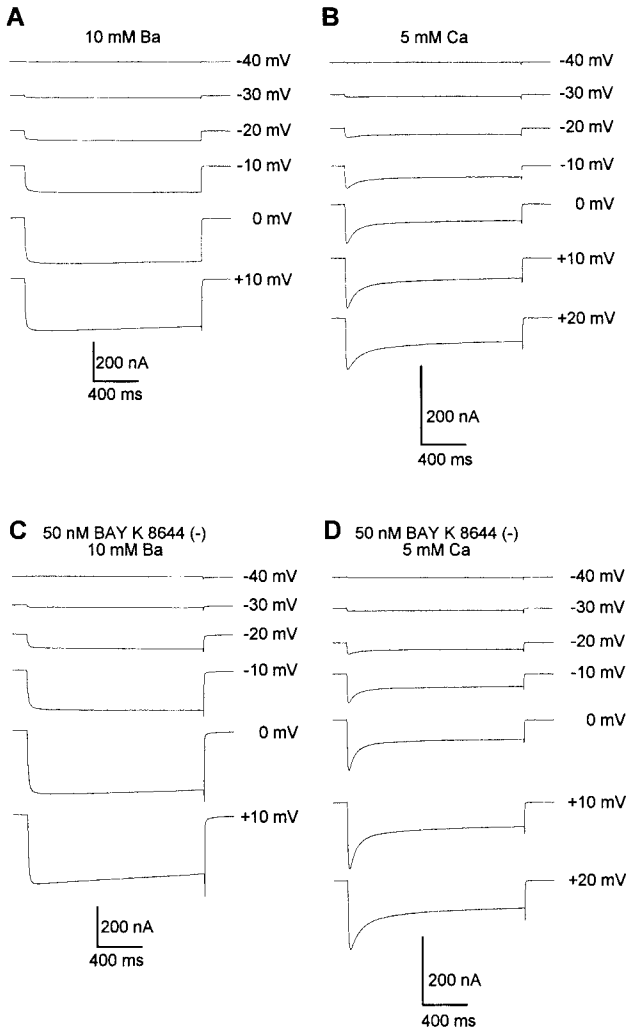

FIGURE 2. Ca^{2+}-dependent inactivation of Ca^{2+} current in the cloned cardiac Ca^{2+} channel $\alpha_{1C}\beta_{2a}$. Superimposed traces evoked in an oocyte expressing α_{1C} and β_{2a} subunits, and the effect of DHP agonist Bay K 8644 (−). The voltage protocol was the same as in Fig. 1. (*A*) Voltage steps from HP −90 mV; Ba^{2+} was the charge carrier (10 mM Ba^{2+}). (*B*) Currents recorded in 5 mM Ca^{2+}. (*C*) Same voltage steps as in *A*, Ba^{2+} currents recorded in the presence of 50 nM Bay K 8644 (−). (*D*) Same voltage steps as in *B*, Ca^{2+} currents recorded in the presence of Bay K 8644 (−). Linear components were digitally subtracted by subpulses from the holding potential using the P/−4 method.

Hadley and Hume, 1987; Campbell et al., 1988; Gutnick et al., 1989; Hadley and Lederer, 1991; Giannattasio et al., 1991), or to a less efficient Ba^{2+}-dependent inactivation process (Ferreira et al., 1997). This voltage-dependent component has not been analyzed here; since its time course is much slower than Ca^{2+}-dependent inactivation, it should not interfere with the main conclusions of this paper.

Voltage and Ca^{2+} dependence of the Inactivation Rates in α_{1C} and $\alpha_{1C}\beta_{2a}$ Currents

The currents in Fig. 3 were recorded in an oocyte expressing the $\alpha_{1C}\beta_{2a}$ Ca^{2+} channel at three different external Ca^{2+} concentrations: 2 (*A*), 5 (*B*), and 10 (*C*) mM Ca^{2+}. Each panel shows currents elicited by three different voltages (holding potential −90 mV), together with superimposed fits to the decay phase of the currents. The inactivating currents were fitted with a double exponential function, yielding to a slow and a fast rate of inactivation. The fast rate depended on external Ca^{2+} concentration, while the slow rate was much less affected by external Ca^{2+} (see also Fig. 6). The peak of the ionic current occurred at +10 mV in 2 mM Ca^{2+}, at +20 mV in 5 mM Ca^{2+}, and at +25 mV in 10 mM Ca^{2+}. The fast rate of inactivation, compared at equivalent voltages corrected for surface charge effect, increased from r_f= 0.0126 ms^{-1} (0 mV, 2 mM Ca^{2+}) to r_f = 0.0224 ms^{-1} (+20 mV, 10 mM Ca^{2+}).

The voltage dependencies of current (I-V) and fast rate of inactivation (r-V) for the experiment in Fig. 3 are shown in Fig. 4 *A* (normalized rates and peak current values). The graph shows a negative voltage shift between the peak of the r-V (*open symbols*) and the peak of the I-V (*filled symbols*). The fact that the peak of the r-V always occurred at more negative voltages than the peak of the I-V suggests a complex dependence of the Ca^{2+} inactivation mechanism on the parameters of channel activation. Possibly, open probability, single channel amplitude, Ca^{2+} influx and accumulation, buffer capacity, and diffusion could be involved. A similar voltage shift between the peak of the r-V and I-V curves was observed in α_{1C} alone (Fig. 4 *B*).

Effect of DHP Agonist Bay K 8644 (−) on α_{1C} and $\alpha_{1C}\beta_{2a}$ Ca^{2+} Currents

The ability of the DHP agonist Bay K 8644 (−) to increase the size of the current by enhancing the open probability, without affecting the single channel amplitude, was used to further investigate the role of the open probability in the Ca^{2+}-dependent inactivation mechanism. We compared the effect of Bay K 8644 (−) on α_{1C} and $\alpha_{1C}\beta_{2a}$ Ca^{2+} currents at three different Ca^{2+} concentrations. Fig. 5 shows $\alpha_{1C}\beta_{2a}$ Ca^{2+} currents elicited by three different voltages, both in the absence (*A*, 2 mM Ca^{2+}) and presence (2, 5, and 10 mM Ca^{2+}, *B–D*, respectively) of Bay K 8644 (−) 500 nM, with the corresponding superimposed fits. The addition of saturating concentration of Bay K 8644 (−) (500 nM) produced a small negative shift of the activation–voltage curve (~5 mV), an approximately twofold increase in the size of the ionic current and a twofold increase in both rates.

Fig. 6 summarizes the effect of external Ca^{2+} and Bay K 8644 (−) on $\alpha_{1C}\beta_{2a}$ Ca^{2+}-dependent rates of inactiva-

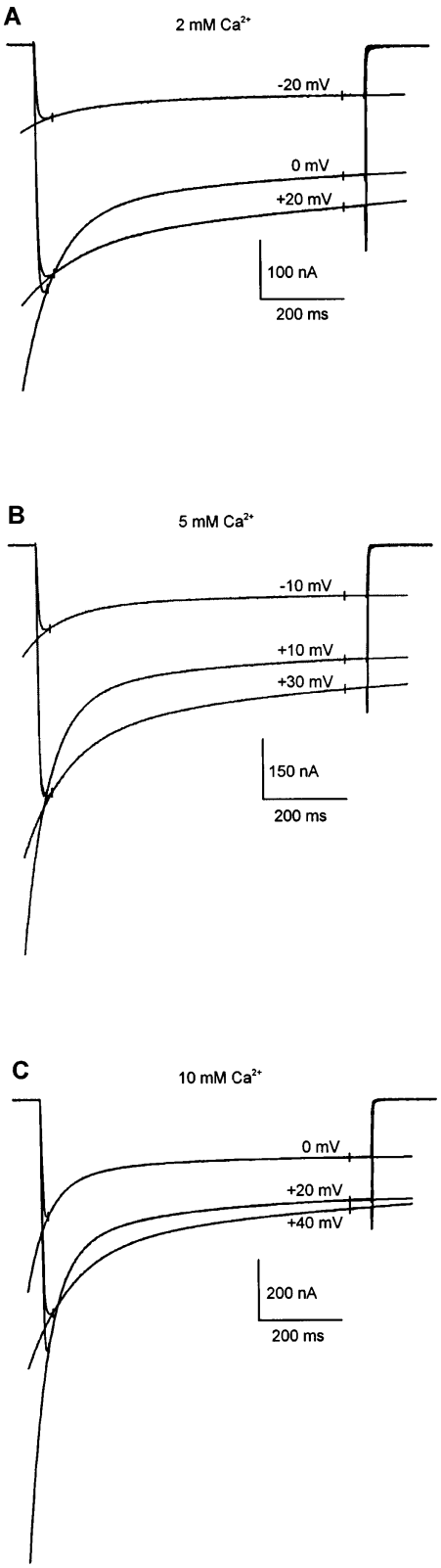

FIGURE 3. Ca^{2+}-dependent inactivation of Ca^{2+} currents in $\alpha_{1C}\beta_{2a}$: effect of different Ca^{2+} concentrations. Superimposed traces evoked in an oocyte expressing $\alpha_{1C}\beta_{2a}$. HP = −90 mV, SHP = −90 mV. (*A*) Voltage steps to −20, 0, +20 mV, in 2 mM Ca^{2+}. The decay phase of the currents were fitted to double exponential functions. The rates of inactivation from the fits were: r_f = 0.0114 ms^{-1}, r_s = 0.0031 ms^{-1} at −20 mV; r_f = 0.0126 ms^{-1}, r_s = 0.0016 ms^{-1} at 0 mV; r_f = 0.0065 ms^{-1}, r_s = not resolved at +20 mV. (*B*) Voltage steps to −10, +10, +30 mV in 5 mM Ca^{2+}. The fitted rates were: r_f = 0.0127 ms^{-1}, r_s = 0.0032 ms^{-1} at −10 mV; r_f = 0.0173 ms^{-1}, r_s = 0.0027 ms^{-1} at +10 mV; r_f = 0.0099 ms^{-1}, r_s = 0.0013 ms^{-1} at +30 mV. (*C*) Voltage steps to 0, −20, +40 mV in 10 mM Ca^{2+}. The fitted rates were: r_f = 0.0202 ms^{-1}, r_s = 0.0039 ms^{-1} at 0 mV, r_f = 0.0224 ms^{-1}, r_s = 0.0035 ms^{-1} at +20 mV, r_f = 0.0092 ms^{-1}, r_s = 0.0008 ms^{-1} at +40 mV.

tion. The maximum value of the fast rates of inactivation in 2 mM Ca^{2+} and in the absence of the DHP agonist was 0.017 ms^{-1} (*diamonds*), and it became 0.038 ms^{-1} in 10 mM Ca^{2+} and in the presence of 500 nM Bay K 8644 (−), thus undergoing a more than threefold overall increase. An equivalent pattern as in Fig. 6 was observed in α_{1C} channels. The slow time constant of the double-exponential inactivation in $\alpha_{1C}\beta_{2a}$ is of the same order of magnitude of the single exponential time constant in α_{1C} alone, and it is Ca^{2+} dependent, as it can be seen in Fig. 6 *A*. Fig. 7 shows the relative position in the voltage axis of the r-V and I-V curves for $\alpha_{1C}\beta_{2a}$ in 5 mM Ca^{2+} and in the presence of 500 nM Bay K 8644 (−).

The same protocol as shown in Fig. 5 for $\alpha_{1C}\beta_{2a}$ currents was applied to α_{1C} alone. In α_{1C} channels, the Ca^{2+} current decay in 2 mM external Ca^{2+} (Fig. 8 *A*) could be fitted to a single exponential function. In α_{1C} alone, the Ca^{2+}-dependent inactivation might be contaminated by the presence of a voltage-dependent inactivation rate recorded in external Ba^{2+} (Fig. 1). However, the addition of Bay K 8644 (−) 500 nM produced the expected negative shift of the activation–voltage curve of ~5 mV together with a significant increase in the size of the current. This current potentiation was associated with a double exponential time course of decay. As expected for a Ca^{2+}-dependent process, the fast component became faster as the Ca^{2+} concentration increased. Taking altogether the results in α_{1C} and $\alpha_{1C}\beta_{2a}$ channels and the action of Bay K 8644 (−) on both channels, we can conclude that both single channel amplitude and open probability participate in the process of Ca^{2+}-dependent inactivation. The effect of the single channel amplitude is reflected by the Ca^{2+} dependence of the inactivation rates and the left shift of the r-V vs. I-V curves, while the role of the open probability is manifested by the faster inactivation rates after facilitating pore opening by the addition of Bay K 8644 (−) and the coexpression of the β_{2a} subunit.

The Effect of BAPTA on Ca^{2+}-dependent Inactivation in $\alpha_{1C}\beta_{2a}$ Currents

To test the accessibility of the site to internal Ca^{2+} buffer, we investigated the effect of perfusing high BAPTA concentration on the Ca^{2+}-dependent inactiva-

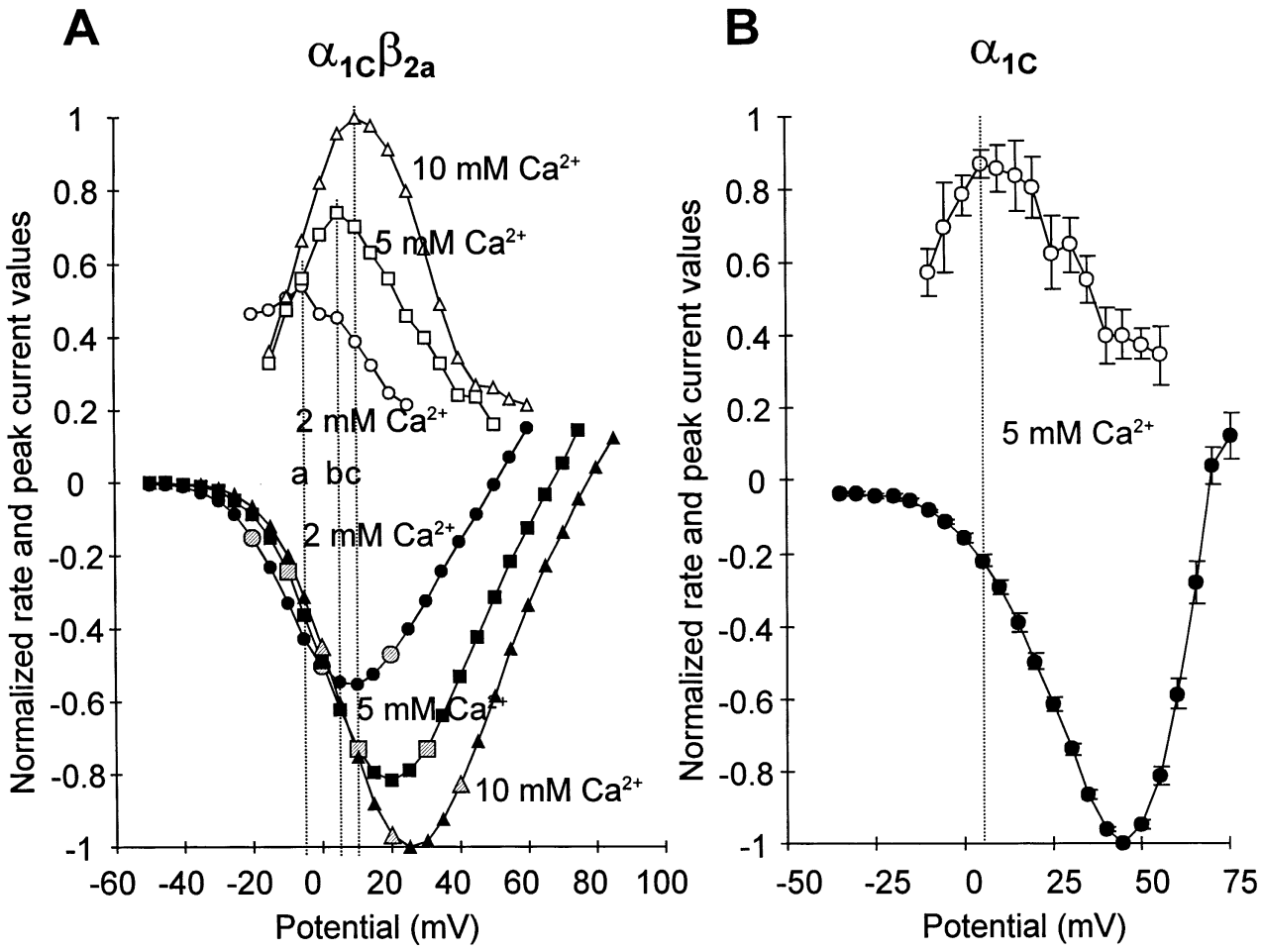

FIGURE 4. Relative positions of the peak currents and the maximal inactivation on the voltage axis in α_{1C} and $\alpha_{1C}\beta_{2a}$. (*A*) Normalized rates and peak current values from the experiment in Fig. 3. Solid symbols are the normalized peak currents (I-V) and open symbols are the normalized rates (r-V) in 2 (○, ●), 5 (□, ■), and 10 (△, ▲) mM Ca^{2+}. The larger symbols on the normalized I-V represent the traces in Fig. 3 (*shaded circles, squares,* and *triangles,* respectively). The dotted lines show the voltage shift between I-V and r-V peaks. The maximal inactivation occurred at 0 (*a*), +10 (*b*), and +15 (*c*) mV in 10 mM Ca^{2+}. The corresponding peaks of the I-Vs were: +10, +20, and +25 mV, respectively. (B) Normalized rates and peak current values in α_{1C} alone in 5 mM Ca^{2+}. The points are mean values ± SEM (n = 7 for the I-V and n = 8 for the r-V). The dotted line shows the voltage shift between I-V and r-V peaks.

tion rates (Fig. 9). The six traces in Fig. 9 *A* have been recorded at different times after the oocyte was mounted and the internal perfusion started (BAPTA 500 mM at the speed of 1 ml/h). Ca^{2+} currents (5 mM Ca^{2+}) were initially contaminated by outward Ca^{2+}-activated Cl^- currents shown as inward slow component and slow tail currents (trace *a*, t = 1 min 15 s). As the perfusion progressed, the Cl^- currents were removed showing the Ca^{2+}-dependent inactivation process. The initial phase of decay in trace *c* (t = 4 min 26 s) could be fitted with a single exponential function (r = 0.0099 ms^{-1}). After 20 min 5 s (trace *f*), the rate of inactivation had become much slower (r = 0.0025 ms^{-1}). The time course of the inactivation rates for the whole experiment is shown in Fig. 9 *B*. During the perfusion, peak current amplitude decreased due to run down. In equivalent prolonged recordings (20 min), when BAPTA was not perfused in the oocyte, the decrease in the size of the current due to run down did not slow down the inactivation rate (Fig. 9, *right*). Fig. 9 *C* shows the progressive run down of the current, while there were no changes in their time course. Fig. 9 *D* shows that the voltage dependence of the fast rate of inactivation at the beginning and after 23 min remained unmodified. Fig. 9 *E* shows small changes in the rates of inactivation during the whole experiment. These results confirm that the internal Ca^{2+} site is accessible to fast Ca^{2+} chelators (Imredy and Yue, 1992; Haack and Rosenberg, 1994), thus ruling out the possibility that this site is located within the conduction pathway.

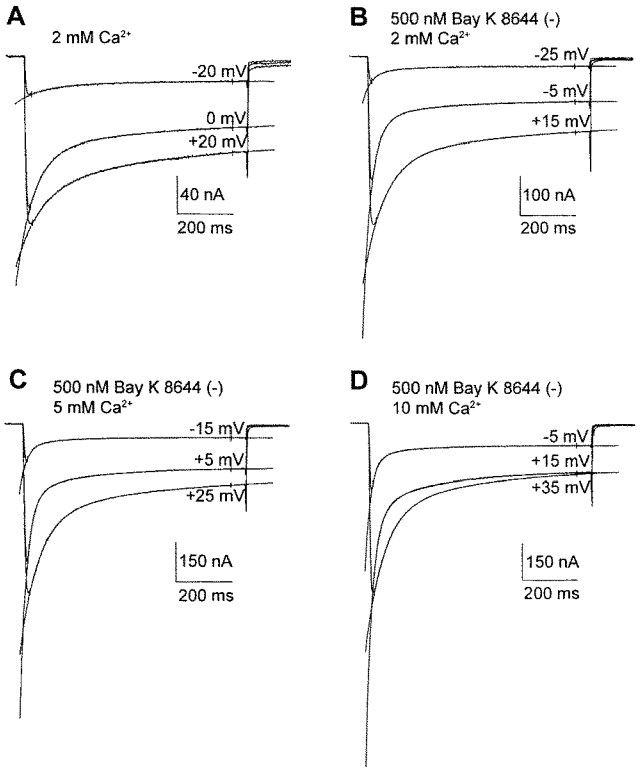

FIGURE 5. Ca^{2+}-dependent inactivation and effect of Bay K 8644 (−) at three different Ca^{2+} concentrations in $\alpha_{1C}\beta_{2a}$. Superimposed traces evoked in an oocyte expressing $\alpha_{1C}\beta_{2a}$. HP = −90 mV, SHP = −90 mV. (*A*) Voltage steps to −20, 0, +20 mV in 2 mM Ca^{2+}. The decay phase of the currents were fitted to double exponential functions. The rates of inactivation from the fits were: r_f = 0.0127 ms^{-1}, r_s = 0.0032 ms^{-1} at −20 mV; r_f = 0.0164 ms^{-1}, r_s = 0.0021 ms^{-1} at 0 mV; r_f = 0.0116 ms^{-1}, r_s = 0.0016 at +20 mV. (*B*) Voltage steps to −25, −5, +15 mV in 2 mM Ca^{2+} and 500 nM Bay K 8644 (−). The fitted rates were: r_f = 0.0333 ms^{-1}, r_s = 0.0056 ms^{-1} at −25 mV; r_f = 0.0336 ms^{-1}, r_s = 0.0045 ms^{-1} at −5 mV; r_f = 0.0132 ms^{-1}, r_s = 0.0016 ms^{-1} at +15 mV. (*C*) Voltage steps to −15, +5, +25 mV in 5 mM Ca^{2+} and 500 nM Bay K 8644 (−). The fitted rates were: r_f = 0.0398 ms^{-1}, r_s = 0.0063 ms^{-1} at −15 mV, r_f = 0.0395 ms^{-1}, r_s = 0.0044 ms^{-1} at +5 mV, r_f = 0.0150 ms^{-1}, r_s = 0.0020 ms^{-1} at +25 mV. (*D*) Voltage steps to −5, +15, +35 mV, in 10 mM Ca^{2+} and 500 nM Bay K 8644 (−). The fitted rates were: r_f = 0.0466 ms^{-1}, r_s = 0.0057 ms^{-1} at −5 mV, r_f = 0.0399 ms^{-1}, r_s = 0.0045 ms^{-1} at +15 mV, r_f = 0.0148 ms^{-1}, r_s = 0.0023 ms^{-1} at +35 mV.

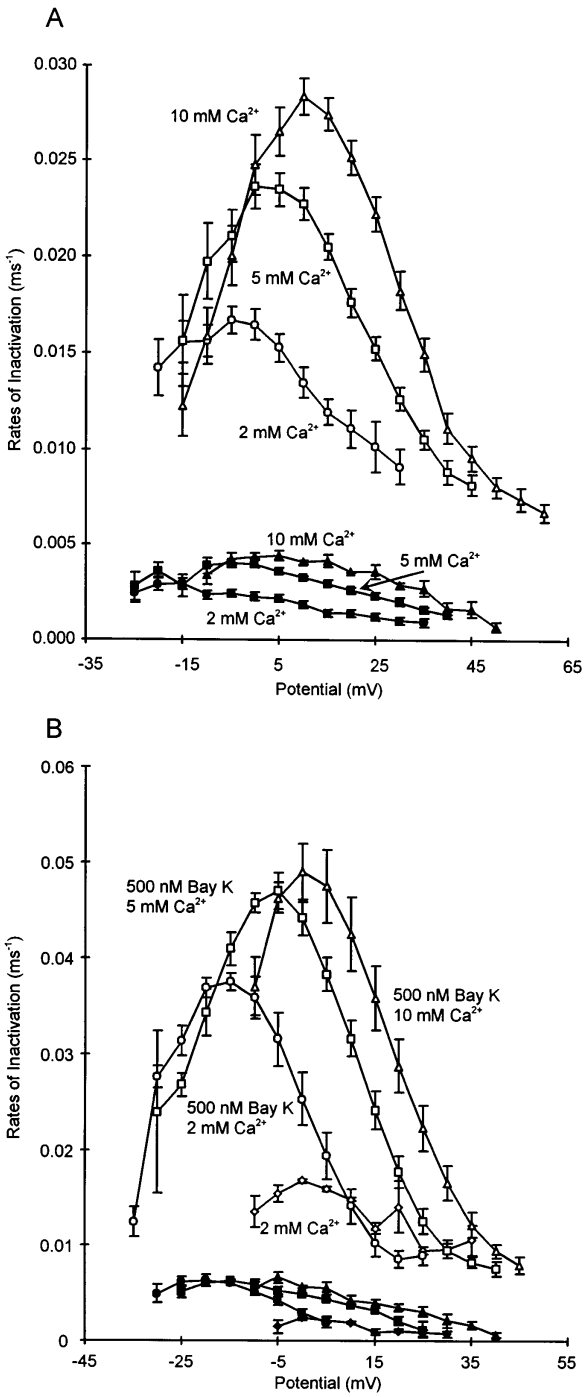

FIGURE 6. Summary plot of the voltage dependence of the fast and slow rates of Ca^{2+}-dependent inactivation in $\alpha_{1C}\beta_{2a}$: effect of Bay K 8644 (−). (*A*) Average values of the fast (*empty symbols*) and slow (*filled symbols*) rates of inactivation in 2 mM Ca^{2+} (○, fast, n = 11; ●, slow, n = 13); 5 mM Ca^{2+} (□, fast, n = 13; ■, slow, n = 14); 10 mM Ca^{2+} (△, fast, n = 16; ▲, slow, n = 13). (*B*) Rates of Ca^{2+}-dependent inactivation in 2 mM Ca^{2+} (◇, fast, n = 10; ◆, slow, n = 8); 2 mM Ca^{2+} + 500 nM Bay K 8644 (−) (○, fast, n = 13; ●, slow, n = 8); 5 mM Ca^{2+} + 500 nM Bay K 8644 (−) (□, fast, n = 15; ■, slow, n = 11); 10 mM Ca^{2+} + 500 nM Bay K 8644 (−) (△, fast, n = 12; ▲, slow, n = 11). All data are shown with their SEMs.

DISCUSSION

We have shown that raising the external Ca^{2+} concentration increased the Ca^{2+}-dependent inactivation rates and left-shifted their voltage dependence: enhancing the Ca^{2+} influx through the channels determined faster decaying currents under conditions in which the open probability should remain unaffected. We also have shown that the rates of Ca^{2+}-dependent inactivation are open probability dependent. Thus, both the single channel amplitude and the open probability contribute to the Ca^{2+}-dependent inactivation mecha-

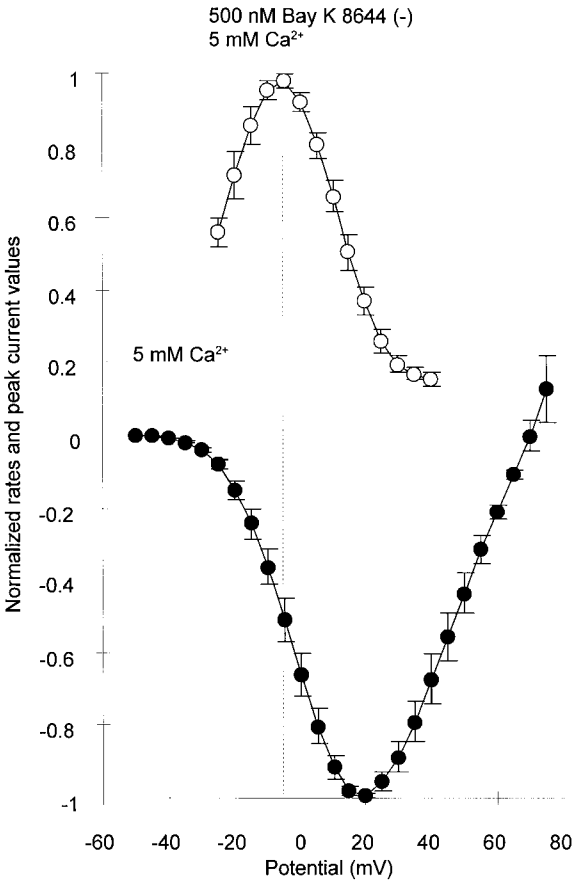

FIGURE 7. Relative positions of the peak currents and the maximal inactivation on the voltage axis in $\alpha_{1C}\beta_{2a}$ in the presence of Bay K 8644 (−). Normalized rates and peak current values in $\alpha_{1C}\beta_{2a}$ in 5 mM Ca^{2+} and in the presence of 500 nM Bay K 8644 (−). The points are mean values ± SEM ($n = 4$ for I-V and $n = 3$ for r-V). The dotted line shows the voltage shift between I-V and r-V peaks.

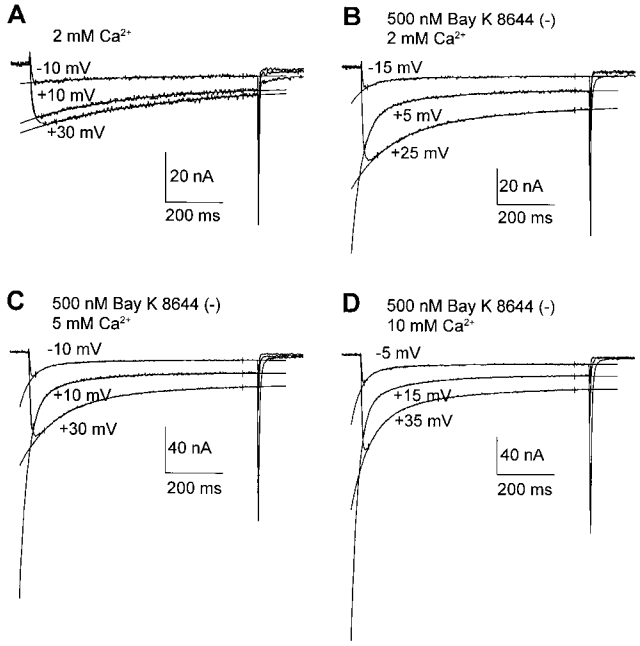

FIGURE 8. Ca^{2+}-dependent inactivation and effect of Bay K 8644 (−) at three different Ca^{2+} concentrations in α_{1C}. Superimposed traces evoked in an oocyte expressing α_{1C}. HP = −90 mV, SHP = −90 mV. (*A*) Voltage steps to −10, +10, +30 mV in 2 mM Ca^{2+}. The decay phase of the currents was fitted to a single exponential function. The rates of inactivation from the fits were: $r = 0.0027$ ms^{-1} at −10 mV, $r = 0.0028$ ms^{-1} at +10 mV, $r = 0.0021$ at +30 mV. (*B*) Voltage steps to −15, +5, +25 mV in 2 mM Ca^{2+} and 500 nM Bay K 8644 (−). The decay phase of the currents were fitted to double exponential functions. The fitted rates were: $r_f = 0.0192$ ms^{-1}, $r_s = 0.0016$ ms^{-1} at −15 mV; $r_f = 0.0277$ ms^{-1}, $r_s = 0.0038$ ms^{-1} at +5 mV; $r_f = 0.0073$ ms^{-1}, $r_s = 0.0007$ ms^{-1} at +25 mV. (*C*) Voltage steps to −10, +10, +30 mV in 5 mM Ca^{2+} and 500 nM Bay K 8644 (−). The fitted rates were: $r_f = 0.0255$ ms^{-1}, $r_s = 0.0038$ ms^{-1} at −10 mV, $r_f = 0.0356$ ms^{-1}, $r_s = 0.0055$ ms^{-1} at +10 mV, $r_f = 0.0079$ ms^{-1}, $r_s = 0.0012$ ms^{-1} at +30 mV. (*D*) Voltage steps to −5, +15, +35 mV in 10 mM Ca^{2+} and 500 nM Bay K 8644 (−). The fitted rates were: $r_f = 0.0299$ ms^{-1}, $r_s = 0.0041$ ms^{-1} at −5 mV, $r_f = 0.0418$ ms^{-1}, $r_s = 0.0053$ ms^{-1} at +15 mV, $r_f = 0.0159$ ms^{-1}, $r_s = 0.0035$ ms^{-1} at +35 mV.

nism. One hypothesis that would explain the dependence of the rates on external Ca^{2+} concentration would be a Ca^{2+} binding site facing the external medium. This possibility is ruled out by the role of internal Ca^{2+} buffers (Lee et al., 1985; Imredy and Yue, 1992; Haack and Rosenberg, 1994) and by recent molecular biology experiments. de Leon et al. (1995) and Zhou et al. (1997) showed that the required region for Ca^{2+}-dependent inactivation in α_{1C} Ca^{2+} channels is located within the COOH terminus of the protein, facing the cytoplasm. The Ca^{2+} binding site could be sensitive to the internal accumulation of Ca^{2+} in a shell underneath the plasma membrane. In this case, the build up of Ca^{2+} would depend on the time integral of the current, the open probability, and the efflux from the shell into the cytoplasm. This mechanism has been proposed and extensively studied for native Ca^{2+} channels (Chad et al., 1984; Lee et al., 1985); it was supported by the dependence of the rates of inactivation on the internal buffer concentration (Lee et al., 1985; Imredy and Yue, 1992; Haack and Rosenberg, 1994) and by observed cross talk among channels (Yue et al., 1990; Mazzanti et al., 1991; Imredy and Yue, 1992). In our case, the shell mechanism becomes unlikely for two reasons: (*a*) only extreme conditions of Ca^{2+} buffering capacity were able to slow down the inactivation process, and (*b*) the lack of observed cross talk among channels. In the oocyte expression, the rates of Ca^{2+} inactivation are independent of the level of expression as shown before by our group (Neely et al., 1994). We have confirmed this finding. In this new set of experiments in $\alpha_{1C}\beta_{2a}$, changes of expression level measured as the peak currents in the I-V curve (from 100–1,200 nA; 2 mM Ca^{2+}) did not affect the predominant fast rate of inactivation, which re-

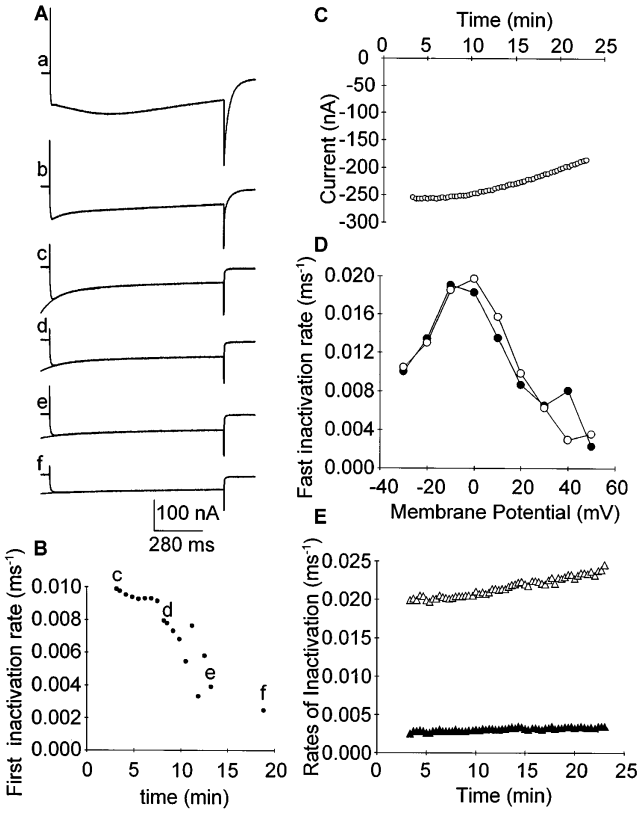

FIGURE 9. Time course of the effect of BAPTA: the removal of Ca^{2+}-dependent inactivation. (*left*) BAPTA-perfused oocyte; (*right*) control oocyte. (*A*) Currents elicited by pulsing to 10 mV from an HP of −90 mV in an oocyte injected with $\alpha_{1C}\beta_{2a}$ (SHP = −90 mV) in the presence of 5 mM Ca^{2+}. The oocyte was perfused with BAPTA 500 mM at the speed of 1 ml/h. *a* was acquired at time *t* = 1 min 15 s; *b* at *t* = 1 min 46 s; *c* at *t* = 4 min 26 s; *d* at *t* = 9 min 48 s; *e* at *t* = 14 min 29 s; *f* at *t* = 20 min 05 s. The initial phase of decay (first 250 ms) in *c*–*f* was fitted to a single exponential. The rates of inactivation were: 0.0099 ms^{-1} (*c*), 0.0077 ms^{-1} (*d*), 0.0039 ms^{-1} (*e*), and 0.0025 ms^{-1} (*f*). (*B*) Time course of the removal of Ca^{2+}-dependent inactivation. Traces in *A* are indicated with the corresponding letters. (*C*) Time course of peak current at 0 mV in 5 mM Ca^{2+} in a control nonperfused oocyte injected with 100 nl of BAPTA 50 mM (see MATERIALS AND METHODS). The control current shows rundown over the time course of the experiment. (*D*) Lack of change in the voltage dependence of the fast rate of the Ca^{2+}-dependent inactivation measured at the beginning (*t* = 0, ●) and at the end of the control experiment (*t* = 23 s, ○). (*E*) Fast (△) and slow (▲) rates of Ca^{2+}-dependent inactivation for the current plotted in *C*, during the time course of the control experiment.

mained between 0.015 and 0.02 ms^{-1} (data not shown). Our results favor a domain mechanism in which the local Ca^{2+} concentration equilibrates in microseconds (Sherman et al., 1990; Shirokov et al., 1993). However, we cannot rule out the possibility that the absence of cross talk was due to the expression level. Under our experimental conditions, it is possible that the expression level was not high enough to reach the critical channel density necessary to the interaction among adjacent channels.

A concern that must be addressed refers to the accessibility of BAPTA to the Ca^{2+} binding site. It is unlikely that the lack of effect on the inactivation rates by the injected BAPTA is due to a slow diffusion in the oocyte cytoplasm. In fact, injections of small quantities of BAPTA or EGTA (Neely et al., 1994) was effective to eliminate the activation of the Ca^{2+}-activated Cl^- channels.

A Minimum Model for Ca^{2+}-dependent Inactivation: Role of the Single Channel Amplitude and Open Probability

Several models have been proposed for Ca^{2+}-dependent inactivation. All these models agree on identifying the Ca^{2+} dependence of the inactivation in one (or more) state-to-state transitions where the rate is dependent on the internal Ca^{2+} concentration. Two main conditions are considered: the "shell" model and the "local domain" model.

In the shell model, the Ca^{2+} flowing through the channels accumulates into a shell underneath the plasma membrane (Standen and Stanfield, 1982; Chad et al., 1984) or it is thought of as charge accumulating on a leaky capacitor (Mazzanti et al., 1991). This assumption leads to second order rates of Ca^{2+}-dependent inactivation where the parameters of channel opening (i.e., single channel conductance and open probability) usually have to be integrated over the variable time.

In the local domain model, the Ca^{2+}-sensing site is located very close to the channel mouth, making it less accessible to chelators, as well as to Ca^{2+} ions coming from adjacent channels. The calculation would thus be restricted to a very small domain surrounding the mouth of the channel, where the Ca^{2+} concentration would reach its steady state value in a few microseconds. This assumption justifies the use of the steady state diffusion equation and results in a linear dependence of the second order rates of inactivation on the single channel amplitude (Sherman et al., 1990; Shirokov et al., 1993).

Both classes of models can account for the main features of the Ca^{2+}-dependent inactivation in L-type Ca^{2+} channels. The domain models also include the possibility of an "extended local domain" in which the volume where the Ca^{2+} concentration is calculated is larger, and a channel can sense the flux of ions that is entering a neighboring channel (cross talk). The fact that Yue et al. (1990) reported that Ca^{2+} entry inactivates the channel it goes through, together with our finding that high concentrations of fast chelators are necessary to reduce the inactivation rates, leads us to test the local domain hypothesis proposed by Sherman et al. (1990). The local domain model has been used with an expanded kinetic scheme to account for the voltage shift between the r-V and I-V curves.

The steady state equation for diffusion in a sphere is, when the diffusion happens only on the radial dimension:

$$C = B + \frac{\phi}{r}, \quad (1)$$

where C is the ion concentration, B is the boundary concentration (in our case, B is the cytoplasmic Ca^{2+} concentration), ϕ is the influx, and r is the radius. Eq. 1 means that, if $[Ca^{2+}]_i$ is the internal Ca^{2+} concentration at rest, then the concentration near the pore will be

$$[Ca^{2+}] = [Ca^{2+}]_i + Ai, \quad (2)$$

where i is the single channel amplitude and A is a constant. The constant A takes into account the diffusion coefficient for Ca^{2+} and the effect of chelators. In a voltage-independent transition from an open state to a Ca^{2+}-inactivated state, the rate will be linearly dependent on the internal Ca^{2+} concentration: $\alpha = \alpha_0[Ca^{2+}]$. Thus, with the assumptions that Ca^{2+} binds instantaneously to a single site and at a fixed distance from the site, the rate of Ca^{2+}-dependent inactivation depends linearly on the flux; i.e., on the single channel amplitude i. The inactivation process will also be open probability dependent since the inactivated state is sequentially connected to the open state.

Then we assumed that the transition rates between all the states in the kinetic model follow the Eyring rate theory; i.e., they are exponential functions of the form:

$$\alpha_i = \alpha_{0i} e^{z_i \delta_i \frac{e^- V}{kT}}$$

$$\beta_i = \beta_{0i} e^{-z_i (1-\delta_i) \frac{e^- V}{kT}},$$

where α_i are the forward rates and β_i are the backward rates. α_{0i} and β_{0i} are the voltage-independent rates:

$$\alpha_{0i} = \frac{kT}{h} e^{-\frac{\Delta W_{if}}{kT}} \text{ and } \beta_{0i} = \frac{kT}{h} e^{-\frac{\Delta W_{ib}}{kT}},$$

where k is the Boltzmann constant (1.38×10^{-23} J/°K, T is the absolute temperature (K), h is the Planck constant (6.63×10^{-34} J s), e^- is the electronic charge (1.602×10^{-19} C), and ΔW_{if} and ΔW_{ib} are the energies required for the transition to occur in the two directions (forward and backward). z_i is the gating charge (e^-), δ_i is the fraction of the electric field sensed by z_i, and V is the membrane voltage. The rates to the Ca^{2+}-inactivated states are voltage independent:

$$\alpha_{Ca^{2+}} = \alpha_{0Ca^{2+}} [Ca^{2+}]$$

$$\beta_{Ca^{2+}} = \beta_{0Ca^{2+}}.$$

Within the above theoretical premises, we started building a kinetic scheme of closed, open, and inactivated states. The computer routine (SCoP) numerically solves the system of differential equations that describes the kinetic scheme, and assigns numbers to the parameters α_{0i}, β_{0i}, z_i, δ_i, $\alpha_{0Ca^{2+}}$, $\beta_{0Ca^{2+}}$. The internal Ca^{2+} concentration, $[Ca^{2+}]$, is calculated as a linear function of the single channel amplitude at each potential.

The kinetic scheme has to satisfy our experimental results, which are summarized as: (*a*) The inactivation is Ca^{2+} dependent: increasing the external Ca^{2+} concentration produces an increase in the absolute values of the rates of inactivation. (*b*) The process is open probability dependent: increasing the open probability with DHP agonist Bay K 8644 (−) or by coexpressing the β_{2a} subunit together with the α_{1C} subunit produces an increase in the rates of inactivation. (*c*) The time course of the decay can be fitted with a double exponential function. The initial fast rate of inactivation is not present (or not detectable) if the α_{1C} subunit is expressed alone and when α_{1C} currents are measured in the absence of Bay K 8644 (−). (*d*) The r-V curve peaks at more negative voltages than the I-V curve.

A sequential model of the form

$$C_1 \cdots C_n \rightleftharpoons O \overset{Ca^{2+}}{\rightleftharpoons} I$$

cannot predict all of these features, specifically it cannot reproduce the observed shift between I-V and r-V. This model predicts that the r-V and the I-V peak at the same potentials under conditions of a fast activation and a slow inactivation (Sherman et al., 1990). If we were to relax these constraints, the decay phase of the current would be less evident due to the slow activa-

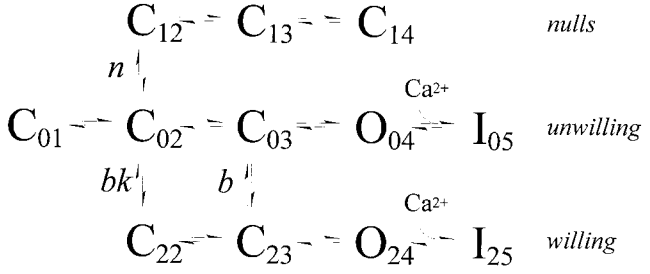

FIGURE 10. Model of Ca^{2+}-dependent inactivation. Three modes of L-type Ca^{2+} channels are originating from a single deep closed state (C_{01}). The top line has no opening: the channel remains silent. The middle and bottom lines end with open states and subsequent Ca^{2+}-dependent inactivated states. The rates (α, β), charges (z), and fractions of the field (δ) that have been used for the fits and simulation are shown in Table I, and they refer to the kinetic transitions as follows: α_{01}, β_{01}, z_1, δ_1: $C_{01} \leftrightarrow C_{02}$; α_{02}, β_{02}, z_2, δ_2: $C_{02} \leftrightarrow C_{03}$; α_{03}, β_{03}, z_3, δ_3: $C_{03} \leftrightarrow O_{04}$; α_{04}, β_{04}: $O_{04} \leftrightarrow I_{05}$, Ca^{2+}-dependent, voltage-independent transition; α_{12}, β_{12}, z_2, δ_2: $C_{12} \leftrightarrow C_{13}$; α_{13}, β_{13}, z_3, δ_3: $C_{13} \leftrightarrow C_{14}$; α_{22}, β_{22}, z_2, δ_2: $C_{22} \leftrightarrow C_{23}$; α_{23}, β_{23}, z_3, δ_3: $C_{23} \leftrightarrow O_{24}$; α_{24}, β_{24}: $O_{24} \leftrightarrow I_{25}$, Ca^{2+}-dependent, voltage-independent transition; α_n, β_n: $C_{02} \leftrightarrow C_{12}$, voltage-independent transition; α_{bk}, β_{bk}: $C_{02} \leftrightarrow C_{22}$, voltage-independent transition; α_b, β_b: $C_{03} \leftrightarrow C_{23}$, voltage-independent transition.

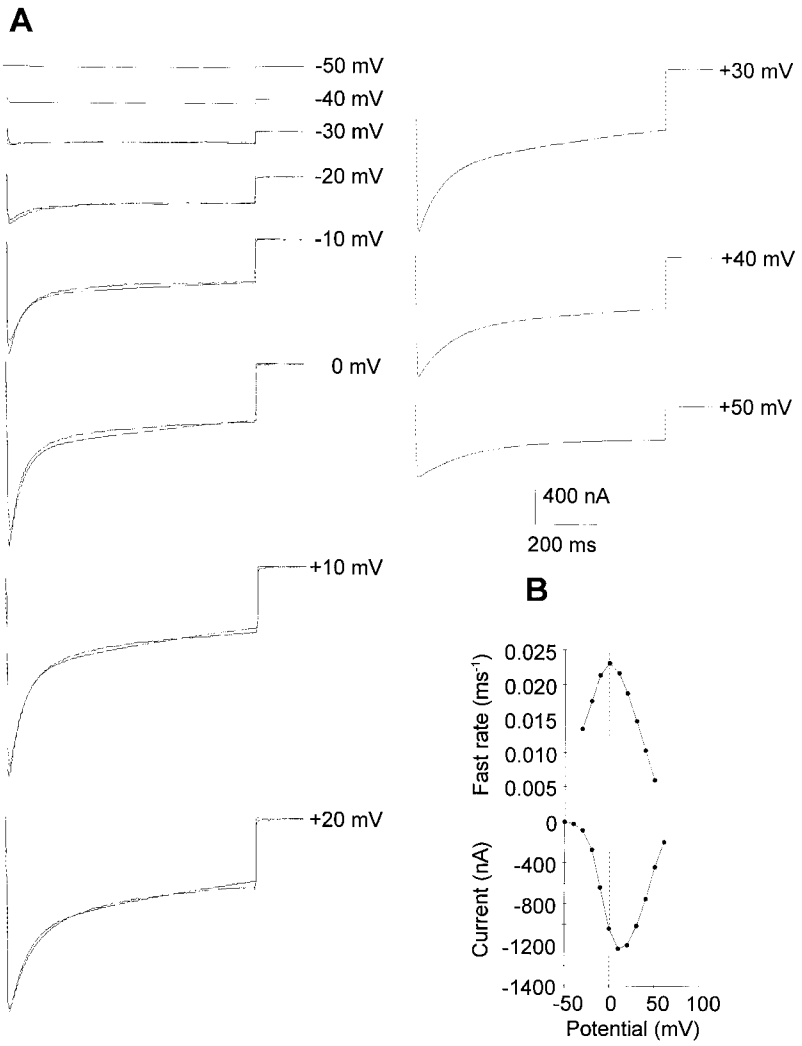

FIGURE 11. Fits and simulations of $\alpha_{1C}\beta_{2a}$ Ca^{2+} currents. (*A*) Current traces recorded from an oocyte expressing $\alpha_{1C}\beta_{2a}$, in response to voltage stimuli of −20, −10, 0, +10, and +20 mV. The traces are superimposed with their fits, generated by the model-fitting procedure described in MATERIALS AND METHODS. (*B*) I-V and r-V are from the simulated traces in *A*. The current peaks at 10 mV, while the r-V peaks at 0 mV. The values for the fast rates of inactivation were obtained by fitting the decay phase of the simulated current with a double exponential function.

tion, and the peak of the r-V would tend to be more positive than the peak of the I-V curve.

We know from single channel data that the α_{1C} and $\alpha_{1C}\beta_{2a}$ Ca^{2+} channels undergo "silent" transitions (i.e., they gate without opening), and they are able to open with different open probability patterns (Costantin et al., 1995). Thus, we have tested the model proposed by Bean (1989) with the modifications shown in Fig. 10. The kinetic scheme has three parallel lines of states that develop as branches from an initial closed state. The parallel transitions carry the same amount of charge. In the top line, the channel never opens, although it displaces all the charge of the voltage sensor. The middle (unwilling) and bottom (willing) lines have final open states connected to final inactivated states. The vertical transitions between the lines are voltage independent and can be Bay K 8644 (−) and β subunit sensitive.

Fig. 11 shows experimental data from an oocyte injected with the $\alpha_{1C}\beta_{2a}$ Ca^{2+} channel together with superimposed fitted traces to the model of Fig. 10. In this model, the rates connecting the open states to the Ca^{2+}-inactivated states consist of a constant coefficient times the local Ca^{2+} concentration, according to Eq. 2 (Table I). The simulated traces in Fig. 11 *B* are shown together with their I-V and r-V curves (fast rate, Fig. 11 *C*). This model predicts the shift between the peaks of the two curves.

Thus, we can conclude that the kinetic scheme in Fig. 10 reproduces well the experimental data for $\alpha_{1C}\beta_{2a}$ channels. In the case of α_{1C} alone, though it is possible to reproduce the main kinetic features of the data, such as the slower activation phase of the currents and the u-shaped voltage dependence of the inactivation rates, the possible presence of a contaminating voltage-dependent inactivation does not allow a clear analysis of the time course of decay. This intrinsic limitation in the modeling of α_{1C} currents would not produce a reliable set of parameters for the kinetic scheme in the case of α_{1C} alone.

In testing the effect of the β_{2a} subunit on α_{1C} Ca^{2+}-dependent inactivation, a possible concern is whether

TABLE I

Fitted Values for the Simulated Currents

$\alpha_{1C}\beta_{2a}$			
Forward voltage-independent coefficient		Backward voltage-independent coefficient	
	ms^{-1}		ms^{-1}
α_{01}	0.0016	β_{01}	0.0001
α_{02}	24.6178	β_{02}	42.5775
α_{03}	0.0001	β_{03}	0.0001
α_{04}	214.2350	β_{04}	0.0001
	$[Ca^{2+}]$		
α_{12}	0.7958	β_{12}	5.9780
α_{13}	0.0910	β_{13}	1.4961
α_{22}	1.0000	β_{22}	1.0000
α_{23}	0.1984	β_{23}	0.1019
α_{24}	1.1180 $[Ca^{2+}]$	β_{24}	0.0001
α_{bk}	1.0000	β_{bk}	0.00727
α_{b}	161.7120	β_{b}	0.67953
α_{n}	3.3940	β_{n}	0.00135
	Charge (e^-)		Fraction of the field
z_1	0.2574	δ_1	0.8246
z_2	0.0001	δ_2	0.0001
z_3	2.9835	δ_3	0.4307

Values of rates, charge, and fraction of the field in each transition for the model illustrated in Fig. 10. The rates are:

$$\alpha_{ij}(V) = \alpha_{ij} e^{\frac{z_j \delta_j eV}{kT}},\ \beta_{ij}(V) = \beta_{ij} e^{\frac{-z_j (1-\delta_j) eV}{kT}}.$$

the endogenous β_{3xo} subunit changed the properties of the α_1 subunits when injected alone. The coexpression β_{3xo} with the α_{1E} and α_{1C} (data not published for α_{1C}) clones produced the generic effect of β subunit of shifting to more negative potential G-V curves (Tareilus et al., 1997). We concluded that the endogenous β_{3xo} has a role in channel expression, but the quantities present are not sufficient to induce kinetic changes.

A further question concerns the molecular mechanism for the Ca^{2+}-dependent inactivation process. Since the Ca^{2+}-sensitive region has been identified within the COOH terminus of the α subunit (de Leon et al., 1995; Zhou et al., 1997), we can speculate that the Ca^{2+} binding to the COOH terminus produces an allosteric change in the conformation of the protein, such as a collapse of the pore. Another possibility is that the COOH terminus, once Ca^{2+} has bound, folds backward and blocks the pore, with a mechanism analogous to the N-type inactivation in *Shaker* K^+ channels (Hoshi et al., 1990). However, if the Ca^{2+} binding site is located in the COOH terminus of the α_{1C} subunit, the COOH terminus could be folded in order for the Ca^{2+} site to be in close proximity to the pore. Differences in the tertiary structure between native and cloned channels that could arise from differences in the folding of the COOH terminus may modify the accessibility of the Ca^{2+} binding site to intracellular Ca^{2+} buffers.

We thank Dr. Ramon Latorre and Dr. Ligia Toro for kindly reading the manuscript and Ms. Jin for injection of *Xenopus laevis* oocytes.

This work was supported by National Institutes of Health (NIH) grant AR-38970 to E. Stefani. N. Qin is the recipient of NIH National Research Service Award GM17120-02 and of the American Heart Association (AHA) Scientist Development Grant 9630053N. This work was done during the tenure of a Grant-in-Aid 113-GI1 award to R. Olcese from the American Heart Association, Greater Los Angeles Affiliate (Los Angeles, CA).

Original version received 28 April 1997 and accepted version received 14 January 1998.

REFERENCES

Barish, M.E. 1983. A transient calcium-dependent chloride current in the immature *Xenopus* oocyte. *J. Physiol. (Camb.).* 342:309–325.

Bean, B.P. 1989. Neurotransmitter inhibition of neuronal calcium currents by changes in channel voltage dependence. *Nature.* 340: 153–156.

Campbell, D.L., W.R. Giles, J.R. Hume, and E.F. Shibata. 1988. Inactivation of calcium current in bull-frog atrial myocytes. *J. Physiol. (Camb.).* 403:287–315.

Chad, J. 1989. Inactivation of calcium channels. *Comp. Biochem. Physiol.* 93:95–105.

Chad, J., R. Eckert, and D. Ewald. 1984. Kinetics of calcium-dependent inactivation of calcium currents in voltage-clamped neurones of *Aplysia californica*. *J. Physiol. (Camb.).* 347:279–300.

Costantin, J.L., N. Qin, L. Birnbaumer, E. Stefani, and A. Neely. 1995. β subunit coexpression induces long channel openings in the α_{1C} cardiac calcium channel. *Biophys. J.* 68:*A*258. (Abstr.)

de Leon, M., Y. Wang, L. Jones, E. Perez-Reyes, X. Wei, T.W. Soong, T.P. Snutch, and D.T. Yue. 1995. Essential Ca^{2+}-binding motif for Ca^{2+}-sensitive inactivation of L-Type Ca^{2+} channels. *Science.* 270: 1502–1506.

Eckert, R., and J. Chad. 1984. Inactivation of Ca channels. *Prog. Biophsy. Mol. Biol.* 44:261–267.

Ferreira, G., J. Yi, E. Rios, and R. Shirokov. 1997. Barium-dependent inactivation of L-type calcium channels. *Biophys. J.* 72:*A*112. (Abstr.)

Galli, A., A. Ferroni, L. Bertollini, and M. Mazzanti. 1994. Inactivation of single Ca^{2+} channels in rat sensory neurons by extracellular Ca^{2+}. *J. Physiol. (Camb.).* 477:15–26.

Giannattasio, B., S.W. Jones, and A. Scarpa. 1991. Calcium currents in the A7r5 smooth muscle-derived cell line. Calcium-dependent and voltage-dependent inactivation. *J. Gen. Physiol.* 98:987–1003.

Gutnick, M.J., H.D. Lux, D. Swandulla, and H. Zucker. 1989. Voltage-dependent and calcium-dependent inactivation of calcium channel current in identified snail neurones. *J. Physiol. (Camb.).* 412:197–220.

Haack, J.A., and R.L. Rosenberg. 1994. Calcium-dependent inacti-

vation of L-type calcium channels in planar lipid bilayers. *Biophys. J.* 66:1051–1060.

Hadley, R.W., and J.R. Hume. 1987. An intrinsic potential-dependent inactivation mechanism associated with calcium channels in guinea-pig myocytes. *J. Physiol. (Camb.).* 389:205–222.

Hadley, R.W., and W.J. Lederer. 1991. Properties of L-type calcium channel gating current in isolated guinea pig ventricular myocytes. *J. Gen. Physiol.* 98:265–285.

Hess, P., J.B. Lansman, and R.W. Tsien. 1984. Different modes of Ca channel gating behaviour favoured by dihydropyridine Ca agonists and antagonists. *Nature.* 311:538–544.

Hoshi, T., W.N. Zagotta, and R.W. Aldrich. 1990. Biophysical and molecular mechanisms of Shaker potassium channel inactivation. *Science.* 250:533–538.

Huang, Y., J.M. Quayle, J.F. Worley, N.B. Standen, and M.T. Nelson. 1989. External cadmium and internal calcium block of single calcium channels in smooth muscle cells from rat mesenteric artery. *Biophys. J.* 56:1023–1028.

Imredy, J.P., and D.T. Yue. 1992. Submicroscopic Ca^{2+} diffusion mediates inhibitory coupling between individual Ca^{2+} channels. *Neuron.* 9:197–207.

Kostyuk, P.G. 1992. Calcium ions in nerve cell function. Oxford Neuroscience Series, 1. Oxford University Press, New York.

Lee, K.S., E. Marban, and R.W. Tsien. 1985. Inactivation of calcium channels in mammalian heart cells: joint dependence on membrane potential and intracellular calcium. *J. Physiol. (Camb.).* 364: 395–411.

Mazzanti, M., L.J. DeFelice, and Y.M. Liu. 1991. Gating of L-type Ca^{2+} channels in embryonic chick ventricle cells: dependence on voltage, current and channel density. *J. Physiol. (Camb.).* 443:307–334.

Miledi, R. 1982. A calcium-dependent outward current in *Xenopus laevis* oocytes. *Proc. R. Soc. Lond. B Biol. Sci.* 215:492–497.

Neely, A., R. Olcese, X. Wei, L. Birnbaumer, and E. Stefani. 1994. Ca^{2+}-dependent inactivation of a cloned cardiac Ca^{2+} channel α_1 subunit (α_{1C}) expressed in *Xenopus* oocytes. *Biophys. J.* 66:1895–1903.

Sherman, A., J. Keizer, and J. Rinzel. 1990. Domain model for Ca^{2+}-inactivation of Ca^{2+} channels at low channel density. *Biophys. J.* 58:985–995.

Shirokov, R., R. Levis, N. Shirokova, and E. Ríos. 1993. Ca^{2+}-dependent inactivation of cardiac L-type Ca^{2+} channels does not affect their voltage sensor. *J. Gen. Physiol.* 102:1005–1030.

Standen, N.B., and P.R. Stanfield. 1982. A binding-site model for calcium channel inactivation that depends on calcium entry. *Proc. R. Soc. Lond. B Biol. Sci.* 217:101–110.

Stefani, E., L. Toro, E. Perozo, and F. Bezanilla. 1994. Gating of *Shaker* K^+ channels: I. Ionic and gating currents. *Biophys. J.* 66: 996–1010.

Tareilus, E., M. Roux, N. Qin, R. Olcese, J. Zhou, E. Stefani, and L. Birnbaumer. 1997. A Xenopus oocyte beta subunit: evidence for a role in the assembly/expression of voltage-gated calcium channels that is separate from its role as a regulatory subunit. *Proc. Natl. Acad. Sci. USA.* 94:1703–1708.

Wei, X., E. Perez-Reyes, A.E. Lacerda, G. Schuster, A.M. Brown, and L. Birnbaumer. 1991. Heterologous regulation of the cardiac Ca^{2+} channel α_1 subunit by skeletal muscle β and γ subunits. Implications for the structure of cardiac L-type Ca^{2+} channels. *J. Biol. Chem.* 266:21943–21947.

Yue, D.T., P.H. Backx, and J.P. Imredy. 1990. Calcium-sensitive inactivation in the gating of single calcium channels. *Science.* 250: 1735–1738.

Zhou, J., R. Olcese, N. Qin, F. Noceti, E. Stefani, and L. Birnbaumer. 1997. Feedback inhibition of calcium channels by calcium depends on a short sequence of the carboxyterminus that does not include the Ca^{2+} binding of a motif with similarity to calcium binding domains. *Proc. Natl. Acad. Sci. USA.* 94:2301–2305.

Zong, X., and F. Hofmann. 1996. Ca^{2+}-dependent inactivation of the class C L-Type Ca^{2+} channel is a property of the α_1 subunit. *FEBS Lett.* 378:121–125.